Article

Assembly of a 3-D cobalt(II) supramolecular framework and its applications in hydrofunctionalization of ketones and aldehydes

Guoqi Zhang [1,*], Alex Wang [1,†], Haisu Zeng, [2] Shengping Zheng,[2] and Michelle C. Neary [2]

[1] Department of Sciences, John Jay College and PhD Program in Chemistry, The Graduate Center, The City University of New York, New York, NY 10019, USA; guzhang@jjay.cuny.edu
[2] Department of Chemistry, Hunter College, The City University of New York, New York, NY 10065, USA
† Current address: Syosset High School, 70 S Woods Rd, Syosset, NY 11791, USA
* Correspondence: guzhang@jjay.cuny.edu

Abstract: A ditopic nitrogen ligand (*E*)-N′-(pyridin-4-ylmethylene)isonicotinohydrazide (**L**) containing both divergent pyridyl coordination sites and a hydrogen-bonding hydrazide-hydrazone moiety was synthesized. The $Co(NCS)_2$-mediated self-assembly of **L** has resulted in the synthesis of a novel 3-dimensional (3-D) supramolecular framework (**1**) that features both coordination and hydrogen bonding interactions. X-ray structural analysis reveals the formation and coordination mode of **1** in the solid state. The rational utilization of coordination bonds and hydrogen bonding interactions is confirmed and responsible for constructing the 3-D materials. Catalytic studies using **1** in the presence of an activator are performed for the hydroboration (or hydrosilylation) reactions of ketones and aldehydes, and the results are compared with previously reported cobalt-based polymeric catalysts.

1. Introduction

The design and synthesis of metal-organic materials with well-defined structural topology and intriguing properties are attracting tremendous attention in recent years [1-3]. Among the driving forces responsible for the formation of novel materials between organic ligands and metal ions, the coordination and hydrogen-bonding interactions are considered to be most important. In general, robust 1-D or 2-D networks can be first constructed by strong metal-organic coordination bonds and then higher dimensional structures will be assembled by hydrogen-bonding interactions [4]. Indeed, such concept has been implemented to the construction of a number of functional metal-organic framework materials that have displayed fascinating properties in gas absorption/storage and catalysis in the past decades [5-8].

Metal-catalyzed hydroboration of unsaturated organic functionalities is one of the most attractive methods for synthesis of alkylboronate esters that could be readily converted into the corresponding alcohols or used for C-C bond coupling reactions [9]. Although stoichiometric methods existed for a long time for the hydroboration of some of functional groups such as carbonyls, nitrile, alkenes and alkynes by borohydride reagents, the chemoselective hydroboration has been a challenge [10,11]. Except the earlier contributions using noble metal catalysts, recent progress has stressed on nonprecious, earth-abundant metals, such as Fe, Co, Ni, Cu, Zn, Mn, V, Al, Mg, etc., and thus far, numerous well-defined molecular complexes based on such base metals have been reported, including those showing good chemo- and regio-selectivity [9,12-24]. In addition, simple based-

catalyzed and non-catalytic hydroboration of carbonyl compounds have been recently 45
disclosed [25,26]. It has been also reported that in the hydroboration of alkenes and al- 46
kynes some species of boranes and borohydrides have played a hidden role in the catalytic 47
cycles [27]. 48

We are particularly interested in the design and synthesis of base metal complexes 49
using pincer-type PNP and NNN ligands and their applications in critical catalytic hy- 50
droboration reactions of alkenes, alkynes and carbonyl compounds [22-24]. Although su- 51
perior catalytic performance using well-defined, discrete complexes of Co, Mn, V and Al 52
as catalysts have been revealed, recent work has indicated that polymeric metal-organic 53
materials assembled from ditopic, purely nitrogen ligands such as 4'-pyridyl-2,2';6',2''-ter- 54
pyridine (tpy) and 4,2';6',4''-tpy upon coordinating with cobalt or iron salts can be used as 55
highly efficient precatalysts for hydroboration of various C=X (X = C, N or O) functional- 56
ities [28-31]. Significantly, it was revealed that the 1-D polymeric chain assembled by 4'- 57
pyridyl-2,2';6',2''-tpy and CoCl$_2$ was an excellent precatalyst for the hydroboration of var- 58
ious carbonyl compounds in the presence of a base activator, potassium *tert*-butoxide 59
(KO^{t}Bu), for the hydroboration of various carbonyl compounds, alkenes and alkynes with 60
high turnover efficiency and notable chemo- and regio-selectivity [28-30]. In addition, a 2- 61
D coordination network of FeCl$_2$ with a 4,2';6',4''-tpy derivative was found to catalyze the 62
hydroboration of ketones and aldehydes in air [31]. In general, such metal precatalysts 63
utilize the rigid tpy ligands to form 1-D polymeric chains and 2-D coordination network, 64
yet the synthesis of higher dimensional materials based on tpy-type ligands have been 65
unsuccessful thus far in our group. 66

Intrigued by the fascinating catalytic properties of 3-D metal-organic framework ma- 67
terials assembled by both coordination and hydrogen bonds, we continued on our catalyst 68
design by moving from tpy ligands to semi-rigid Schiff base ligands that contain both 69
pyridine coordination sites and hydrogen bonding moiety. Thus, the structurally simple 70
and synthetically facile ligand, **L** (Scheme 1), was designed in order to obtain novel metal- 71
organic framework structures upon coordinating with octahedral metal ions such as co- 72
balt(II). We have previously studied the fundamental coordination chemistry of similar 73
ligands containing a hydrazide-hydrazone structural unit that can potentially form hy- 74
drogen bonding networks [32,33]. Herein, we report the synthesis and structural charac- 75
terization of a 3-D supramolecular framework (**1**) assembled by **L** and Co(NCS)$_2$ and its 76
catalytic applications in chemoselective hydroboration and hydrosilylation of ketones and 77
aldehydes. 78

79
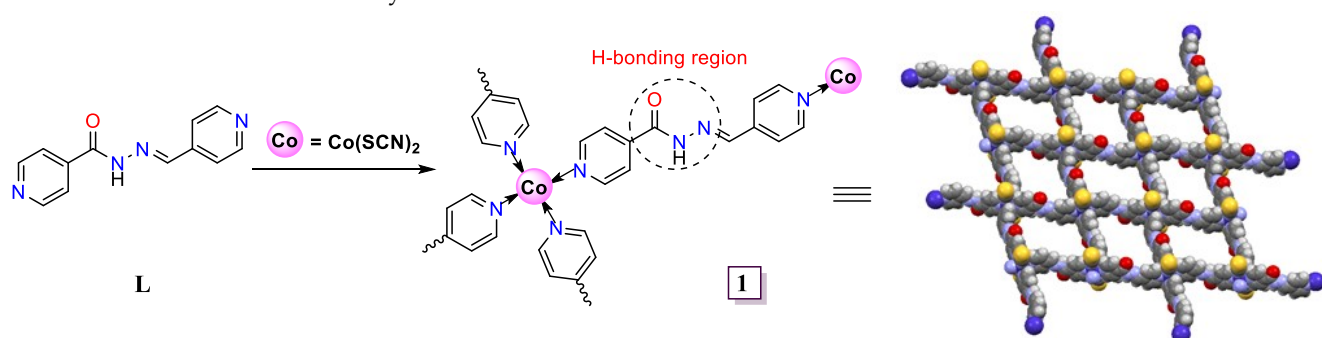
Scheme 1. Schematic representation of the assembly of 2-D grid-like network found in 1 from ligand 80
L and Co(NCS)$_2$. 81

82

2. Materials and Methods 83

2.1. Materials 84

Anhydrous grade solvents and liquid reagents used were obtained from Sigma-Aldrich and Fisher Scientific and stored over 4 Å molecular sieves. FT-IR spectra were recorded on a Shimadzu 8400S instrument with solid samples under N_2 using a Golden Gate ATR accessory. Elemental analysis was performed by the Midwest Microlab LLC at Indianapolis, US. Powder X-ray diffraction (PXRD) was performed with a Bruker D8 Discover microdiffractometer with the General Area Detector Diffraction System (GADDS) equipped with a VANTEC-2000 2D detector. GC-MS analysis was obtained using a Shimadzu GCMS-QP2010S gas chromatograph mass spectrometer. Ligand **L** was prepared according to the literature procedure [34,35].

2.2. Synthesis of *1*

A solution of (*E*)-N′-(pyridin-4-ylmethylene)isonicotinohydrazide (**L**, 113 mg, 0.5 mmol) in CH_2Cl_2/MeOH (2 : 1, v/v, 15 mL) was placed in a test tube. MeOH (5.0 mL) was layered carefully on the top of the first solution, followed by a layer of a solution of $Co(SCN)_2$ (87.5 mg, 0.5 mmol) in MeOH (10 mL). The tube was capped and allowed to stand for one week at room temperature, during which period pale pink crystals suitable for single-crystal X-ray diffraction had formed on the walls of the tube and were isolated by decanting the solvent. The crystals were washed with MeOH and then dried in the air. Yield: 134 mg (86% based on **L**). FT-IR (solid, cm^{-1}): 3207m, 2049s, 1657s, 1613s, 1548s, 1493w, 1293s, 1223m, 1147w, 1115w, 1066s, 1014s, 948m, 816s, 657s. Anal. Calc. for $C_{26}H_{20}CoN_{10}O_2S_2 \cdot CH_3OH$, C 49.17, H 3.67, N 21.24%; Found C 49.07, H 3.99, N 20.95%.

2.3. General Procedure for *1*-Catalyzed Hydroboration of Ketones and Aldehydes

In a glovebox under nitrogen atmosphere, **1** (0.63 mg, 1.0 μmol, based on $Co(\mathbf{L})_2(NCS)_2$) and KO^tBu (1.1 mg, 10 μmol) was placed in a 1.8 mL disposable vial equipped with a stir bar. Ketone or aldehyde (1.0 mmol) and pinacolborane (HBpin, 140.8 mg, 1.1 mmol) were then added. The reaction mixture was allowed to stir at room temperature for 2 h. At completion of the reaction, the reaction was exposed to the air and diethyl ether (10 mL) was added. The crude mixture was treated with 2N NaOH (1 mL) and 30% H_2O_2 (1 mL) stirred at room temperature for 1 h. The solution was extracted with ethyl acetate and washed with brine and water. The organic phase was concentrated under reduced pressure and then purified through a flash column chromatography with SiO_2 using ethyl acetate/hexane as an eluent. The products were characterized by ^1H and ^{13}C NMR spectroscopies.

2.4. General Procedure for *1*-Catalyzed Hydrosilylation of Ketones and Aldehydes

In a glovebox under nitrogen atmosphere, **1** (0.63 mg, 1.0 μmol, based on $Co(\mathbf{L})_2(NCS)_2$) and KO^tBu (1.1 mg, 10 μmol) was placed in a 1.8 mL disposable vial equipped with a stir bar. Ketone or aldehyde (1.0 mmol) and phenylsilane (PhSiH₃, 119.0 mg, 1.1 mmol) were then added. The reaction mixture was allowed to stir at room temperature for 2 h. At completion of the reaction, the reaction was exposed to the air and diethyl ether (10 mL) was added. The crude mixture was treated with 2N NaOH (1 mL) at room temperature for 2 h. The solution was extracted with ethyl acetate and washed with brine and water. The organic phase was concentrated under reduced pressure and then purified through a flash column chromatography with SiO_2 using ethyl acetate/hexane as an eluent. The products were characterized by ^1H and ^{13}C NMR spectroscopies.

2.5. General Procedure for *1*-Catalyzed Chemoselective Hydroboration

In a glovebox under nitrogen atmosphere, **1** (0.63 mg, 1.0 μmol, based on $Co(\mathbf{L})_2(NCS)_2$) and KO^tBu (1.1 mg, 10 μmol) was placed in a 1.8 mL disposable vial equipped with a stir bar. Ketone (1.0 mmol), another reducible substrate (1.0 mmol) and HBpin (128 mg, 1.0 mmol) were then added. The reaction mixture was allowed to stir at room temperature for 2 h. At completion of the reaction, the reaction was exposed to the

air and the solvent was evaporated. The hydroborated product was analyzed by GC-MS   134
using hexamethylbenzene as an internal standard to determine the yield.   135

2.6. X-ray crystallography   136

   A grey-pink crystal of **1** was mounted on a Cryoloop with Paratone-N oil and data   137
were collected at 100 K with a Bruker APEX II CCD using Mo Kα radiation generated   138
from a rotating anode. Data were corrected for absorption with SADABS (Version 2012/1)   139
and the structure was solved by direct methods. All non-hydrogen atoms were refined   140
anisotropically by full matrix least squares on F^2 with SHELXL (Version 2018/3) [36,37].   141
Hydrogen atom H3 on nitrogen atom N3 was found from a Fourier difference map. U_{iso}(H)   142
was set to 1.20 of U_{eq}(N), and the N3-H3 distance was refined using a DFIX command set   143
to 0.87(1) Å [final distance refined to 0.867(10) Å]. All other hydrogen atoms were placed   144
in calculated positions with appropriate riding parameters. The unit cell contained an un-   145
known number of CH$_2$Cl$_2$ and/or MeOH molecules in two separate voids in the unit cell   146
(each was 325 Å^3 with 75 electrons). These were treated as a diffuse contribution to the   147
overall scattering without specific atom positions by SQUEEZE/PLATON [38,39]. The   148
crystal structure was drawn with XP, and packing figures were drawn with the program   149
Mercury v. 3.10.3. Crystallographic data for **1**: C$_{26}$H$_{20}$CoN$_{10}$O$_2$S$_2$, M = 627.57, grey-pink   150
block, monoclinic, space group $P2_1$/c, a = 8.1335(12), b = 24.670(3), c = 9.4320(13) Å, β =   151
91.608(5), U = 1891.8(4) Å^3, Z = 2, Z' = 0.5, D_c = 1.102 Mg m^{-3}, μ(Mo-Kα) = 0.597 mm^{-1}, λ =   152
0.71073 Å, T = 100(2) K. There were 22705 measured, 3583 unique, and 2817 observed [I 153
>2σ(*I*)] reflections. Refinement of reflections with I >2σ(*I*) (190 parameters, 1 restraint) con-   154
verged at R_1 = 0.0395 (R_1 all data = 0.0572), wR_2 = 0.858 (wR_2 all data = 0.0919), GOF = 1.029.   155
CCDC No. 1978581 contains the supplementary crystallographic data for this paper. These   156
data can be obtained free of charge via https://www.ccdc.cam.ac.uk/structures/, or from   157
the Cambridge Crystallographic Data Centre, 12 Union Road, Cambridge CB2 1EZ, UK;   158
fax: (+44) 1223-336-033; or e-mail: deposit@ccdc.cam.ac.uk.   159

3. Results   160

3.1. Synthesis and structural characterization.   161

   The synthesis of ligand **L** was readily carried out in high yield by using a simple   162
Schiff base condensation between isonicotinoyl hydrazide and pyridine-4-carbaldehyde.   163
Previously, this ligand has been utilized for the construction of mixed-ligand Zn and Cd   164
metal-organic frameworks where the hydrazide-hydrazone moiety played an important   165
role for fluorescent metal ion sensing and CO$_2$ absorption [34,35]. The cobalt-directed self-   166
assembly of **L** with Co(NCS)$_2$ was conducted by a layering method in a CH$_2$Cl$_2$/MeOH   167
solution. The block-like crystalline materials of **1** was obtained in 86% yield after one week   168
and the product was isolated by decanting the solvent and then washed with methanol   169
and dried in the air. It was found that the large blocks of **1** tended to lose co-crystallized   170
solvents readily upon exposure to the air, while being cracked into microcrystalline ma-   171
terials. Single-crystal X-ray diffraction analysis was, therefore, carried out with a crystal   172
collected rapidly from the solution and covered with paratone oil to avoid solvent loss   173
from the lattice. Indeed, although its main structure could be unambiguously determined,   174
there are a number of solvent molecules (CH$_2$Cl$_2$ and MeOH) in the unit cell that could   175
not be well refined and hence treated with the program SQUEENE/PLATON [38,39]. The   176
as-dried micro-crystalline sample was characterized by FT-IR and elemental analysis, as   177
well as PXRD analysis. A comparison of the IR spectra between **L** and **1** revealed slight   178
shifts of major absorptions upon coordination, except for the appearance of the character-   179
istic absorption of NCS group at 2053 cm^{-1} (see SI). Elemental analysis confirmed the com-   180
position of **1** with an empirical formula of Co(**L**)$_2$(NCS)$_2$ containing one molecule of MeOH   181
in each repeating unit. The PXRD measurement of the as-dried crystals revealed the par-   182
tial loss of its crystallinity and a pattern distinct from that simulated from single-crystal   183

diffraction data, indicating the possibility of a phase transition, which are frequently observed in porous metal-organic framework [40-42].

In our strategy, the octahedron-coordinating cobalt(II) ions are expected to bind with the terminal pyridyl-N atoms to form a 2-D supramolecular architecture, while leaving the bridging hydrazide-hydrazone area available for the further assembly by 2-D coordination sheets via hydrogen bonding interactions (Scheme 1). Accordingly, X-ray structural analysis of **1** confirms that a novel 3-D framework is constructed through 2-D sheet-like assembly by coordination bonds between **L** as linkers and octahedral $CoN_4(NCS)_2$ as the nodes followed by anticipated hydrogen bonds of the hydrazide-hydrazone regions.
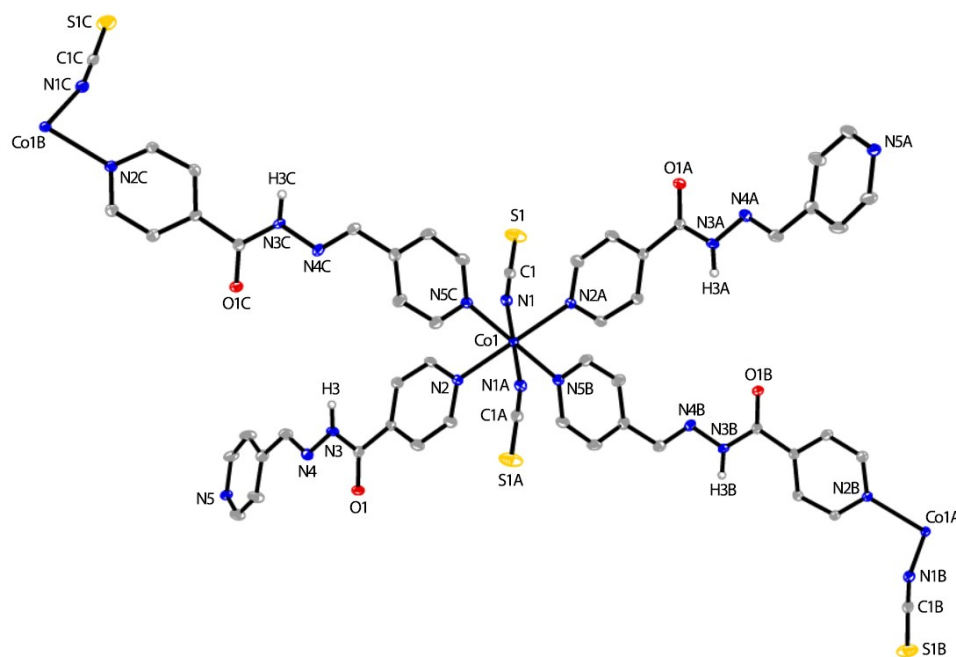
Figure 1. The ORTEP representation of **1** with thermal ellipsoids plotted at the 30% probability level. Hydrogen atoms bound to carbon are omitted for clarity.

1 crystallizes in the monoclinic space group *P*2(1)/c and its ORTEP structure showing the metal coordination environment is represented in Fig. 1. The asymmetric unit contains one independent ligand molecule, 0.5 cobalt centers and one of the thiocyanate ions. Structural expansion around the metal center leads to the formation of a hexa-coordinate Co^{II} center. Each Co^{II} is surrounded by four ligand molecules to form a CoN_6 sphere, and the resultant $Co-N_{pyridyl}$ distances are 2.1760(18) and 2.2203(17) Å, while the $Co-N_{NCS}$ bond is slightly shorter (2.058(2) Å). The adjacent N-Co-N angles are in the range between 87.04(7) and 92.96(7)°, with the cobalt ion residing at an almost perfect octahedral coordination environment (Fig. 1). Further inspection of the structure found that each ligand bonds to two cobalt centers by the end pyridyl sites, thus linking the metal centers to form a 2-D sheet-like network that contains large grids (Fig. 2a). In each grid structure, the adjacent Co…Co distance is 15.440 Å, while the diagonal Co…Co distances are 24.670 and 18.573 Å, respectively, due to the slightly bending conformation of L. Interestingly, the 2-D network was further assembled to a 3-D architecture through inter-layer hydrogen bonding interactions using the hydrazide-NH as an H-bonding donor and C=O as the H-bonding acceptor (N…O = 2.827(2) Å, < N-H…O = 167(2)°), as shown in Fig. 2b. Such a hydrogen bonding packing mode using the central zone of the ligands results in more condensed 3-D molecular stacking, while forming small channels in the crystals with a dimension of ca. 7 × 7 Å, which are mainly occupied by diffused solvents that rapidly evaporate in the air and can be further removed under vacuum.
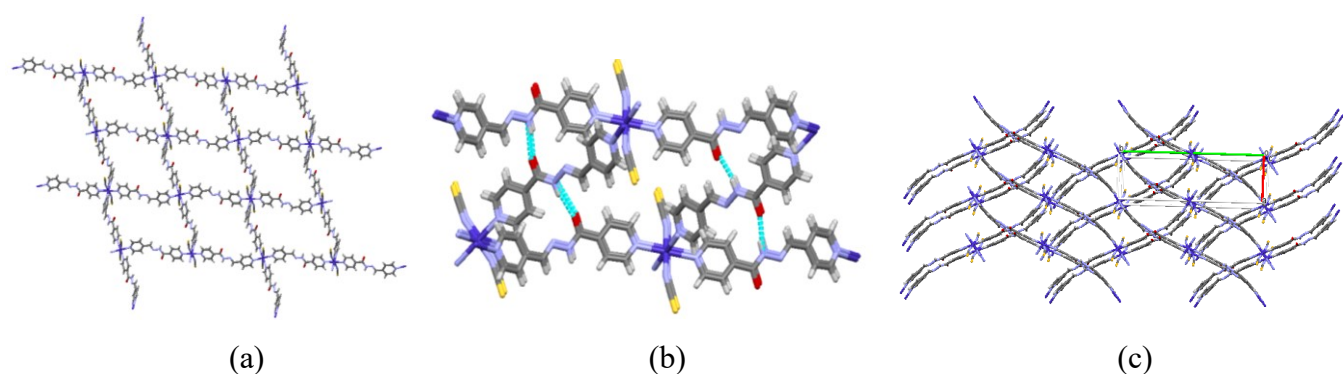
(a)   (b)   (c)

Figure 2. (a) The capped-stick representation of the partial 2-D sheet-like coordination network. (b) The local ball-stick representation showing the interlayer N-H…O hydrogen bonding interactions drawn in green dashed lines. The grid in mid-layer is shown in blue. (c) The The 3-D packing mode of **1** along the crystallographic c axis showing the void molecular channels (diffused solvents are removed for clarification).

3.2. Catalytic applications.

Next, we evaluated the catalytic performance of the 3-D material **1** as a precatalyst for the hydroboration of ketone and aldehyde. First, acetophenone was chosen as a model substrate to react with the hydride source, pinacolborane (HBpin), in the presence of **1** and a base additive, the conditions adopted from the 1-D Co coordination polymer ([Co(4-pytpy)Cl$_2$]$_n$) catalyzed hydroboration previously reported [28]. The results for the screening of reaction conditions are summarized in Table 1. It was revealed that the reaction of acetophenone with HBpin (1.1 eq.) did not proceed in the presence of **1** (0.1 mol% based on one Co(**L**)$_2$(NCS)$_2$ unit) without the addition of an activator (entry 1). Likewise, the reaction gave only a trace amount of product in the presence of KO^{t}Bu (1 mol%) alone as detected by GC-MS analysis (entry 2). In contrast, when the Co(NCS)$_2$ salt combined with KO^{t}Bu was used, moderate yield was observed (entry 3). The combination of **1** and KO^{t}Bu was, therefore, crucial for the formation of active catalytic species and to this end, a quantitative yield of the desired boronate ester was obtained in THF at room temperature (entry 4). The results are identical to those obtained with [Co(4-pytpy)Cl$_2$]$_n$ as a precatalyst (entry 5). The reactivity of the present catalyst is comparable to the reported 1-D cobalt coordination polymer. We further studied the effect of different solvents for this reaction (entries 6-9). It was found that although benzene and toluene were less ideal solvent, pentane and diethyl ether are viable solvents that rendered the reaction with slightly lower yield. It was also delightfully observed that the reaction can proceed equally well without the use of solvent (entry 10), indicating the promising applications of this catalyst in green chemistry [13,31]. We also investigated the effect of additives as it is necessary for the present catalysis. Replacing KO^{t}Bu with KOH, K$_2$CO$_3$, NaBF$_4$ or NaBH$_4$ generally resulted in lower yields of the boronate ester (entries 11-14). However, the strong base, lithium bis(trifluoromethane)sulfonimidate (LiNTf$_2$), was found to facilitate the reaction with comparable results (entry 15).

Table 1. Catalytic test for **1**-catalyzed hydroboration of acetophenone with HBpin.[a.]

Entry	Catalyst	Activator	Solvent	Yield /%[b]
1	**1**	-	THF	0
2	none	KO^{t}Bu	THF	<5
3	Co(NCS)$_2$	KO^{t}Bu	THF	68
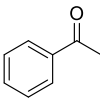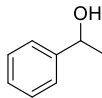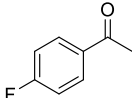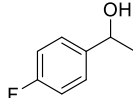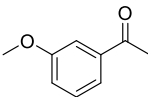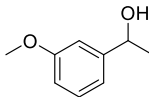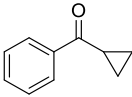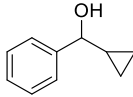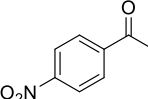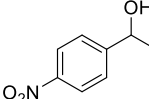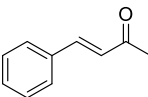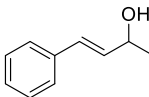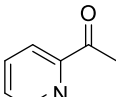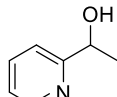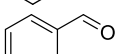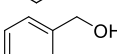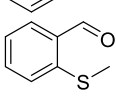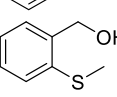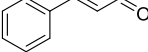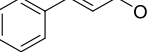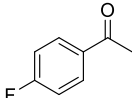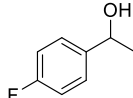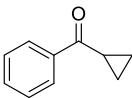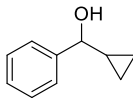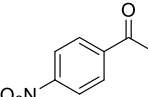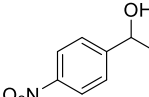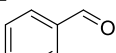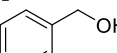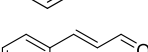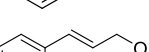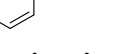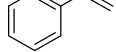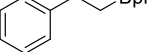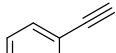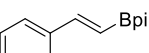
4	**1**	KO*t*Bu	THF	99	
5	[Co(4-pytpy)Cl₂]ₙ	KO*t*Bu	THF	99	
6	**1**	KO*t*Bu	Et₂O	95	
7	**1**	KO*t*Bu	toluene	80	
8	**1**	KO*t*Bu	benzene	86	
9	**1**	KO*t*Bu	pentane	95	
10	**1**	KO*t*Bu	none	99	
11	**1**	KOH	none	58	
12	**1**	K₂CO₃	none	67	
13	**1**	NaBH₄	none	85	
14	**1**	NaBF₄	none	18	
15	**1**	LiNTf₂	none	96	

[a] Conditions: acetophenone (1.0 mmol), HBpin (1.1 mmol, 1.1 eq.), **1** (0.1 mol%), activator (1 mol%) and solvent (0.5 mL), rt, 2 h. [b] Determined by GC-MS analysis with hexamethylbenzene as an internal standard.

Encouraged by the high catalytic activity found for the combined catalyst of **1**/KO*t*Bu under neat and mild conditions, we explored its application for a range of ketones and aldehydes. The results are shown in Table 2. Acetophenone bearing electro-withdrawing and -donating groups, or the bulkier phenyl isopropyl ketone furnished the reaction with high yields of the corresponding boronate esters under neat conditions and secondary alcohols could be readily obtained by hydrolysis (entries 2-5). In addition, α, β-unsaturated ketone and heterocyclic ketone are both suitable substrates for hydroboration, affording the corresponding alcohols with 90% and 82% yield, respectively (entries 6 and 7). Furthermore, aldehydes are also found to hydroborated effectively in the presence of **1**/KO*t*Bu under neat conditions (entries 8-10). Primary alcohols could be isolated upon hydrolysis of the boronate esters with 86-90% yields. We are also interested to see whether other hydride sources can be used for the reduction of ketone and aldehyde. Thus, the popularly used hydride, phenylsilane (PhSiH₃), was tested for the relevant hydrosilylation catalysis. It was delightful to find that both ketones and aldehydes proceed well for hydrosilylation with PhSiH₃ under neat conditions, and the corresponding alcohol products were isolated in 84-92% yields after hydrolysis (entries 11-15). Finally, we tried to expand the applications of this catalyst system for the hydroboration or hydrosilylation of alkenes and alkynes. Unfortunately, the results reveal that the present catalyst is almost inactive for such substrates for both types of hydrofunctionalizations (entries 16-18). This is, however, in contrast with the previously reported tpy-based cobalt(II) coordination polymer that is highly efficient catalyst for the regioselective hydroboration of both polar and non-polar unsaturated bonds [28,29]. These results indicate that the influence of the ligand on the catalytic activity/selectivity. Despite the polymeric nature of **1**, the catalyst system appeared to be homogeneous solution under the catalytic conditions (in the presence of KO*t*Bu and HBpin) and we were unable to recycle the catalyst as a solid by filtration or centrifugation of the reaction mixture, indicating the polymeric structure might have decomposed. At this point, the hidden role played by a borane formed in the reaction mixture and borohydride could not be excluded [27].

Table 2. Catalytic hydroboration or hydrosilylation of ketones and aldehydes using **1** as a precatalyst.[a]

Entry	Substrate	Hydride	Product	Yield (%)[b]

1	(structure: acetophenone)	HBpin	(structure: 1-phenylethanol)	92
2	(structure: 4-fluoroacetophenone)	HBpin	(structure: 1-(4-fluorophenyl)ethanol)	94
3	(structure: 3-methoxyacetophenone)	HBpin	(structure: 1-(3-methoxyphenyl)ethanol)	92
4	(structure: cyclopropyl phenyl ketone)	HBpin	(structure: cyclopropyl(phenyl)methanol)	95
5	(structure: 4-nitroacetophenone)	HBpin	(structure: 1-(4-nitrophenyl)ethanol)	89
6	(structure: benzylideneacetone)	HBpin	(structure: 4-phenyl-3-buten-2-ol)	90
7	(structure: 2-acetylpyridine)	HBpin	(structure: 1-(pyridin-2-yl)ethanol)	82
8	(structure: benzaldehyde)	HBpin	(structure: benzyl alcohol)	88
9	(structure: 2-(methylthio)benzaldehyde)	HBpin	(structure: (2-(methylthio)phenyl)methanol)	90
10	(structure: cinnamaldehyde)	HBpin	(structure: cinnamyl alcohol)	86
11	(structure: 4-fluoroacetophenone)	PhSiH₃	(structure: 1-(4-fluorophenyl)ethanol)	92
12	(structure: cyclopropyl phenyl ketone)	PhSiH₃	(structure: cyclopropyl(phenyl)methanol)	90
13	(structure: 4-nitroacetophenone)	PhSiH₃	(structure: 1-(4-nitrophenyl)ethanol)	84
14	(structure: benzaldehyde)	PhSiH₃	(structure: benzyl alcohol)	85
15	(structure: cinnamaldehyde)	PhSiH₃	(structure: cinnamyl alcohol)	90
16	(structure: styrene)	HBpin	(structure: Bpin addition product)	5 [c]
17	(structure: phenylacetylene)	HBpin	(structure: vinyl Bpin product)	3 [c]
18	(structure: styrene)	PhSiH₃	(structure: SiH₂Ph addition product)	trace [c]

[a] Conditions: substrate (1.0 mmol), HBpin or PhSiH₃ (1.1 mmol, 1.1 eq.), **1** (0.1 mol%), KOᵗBu (1 mol%), neat, rt, 2 h. [b] Isolated yields. [c] Yields determined by GC analysis.
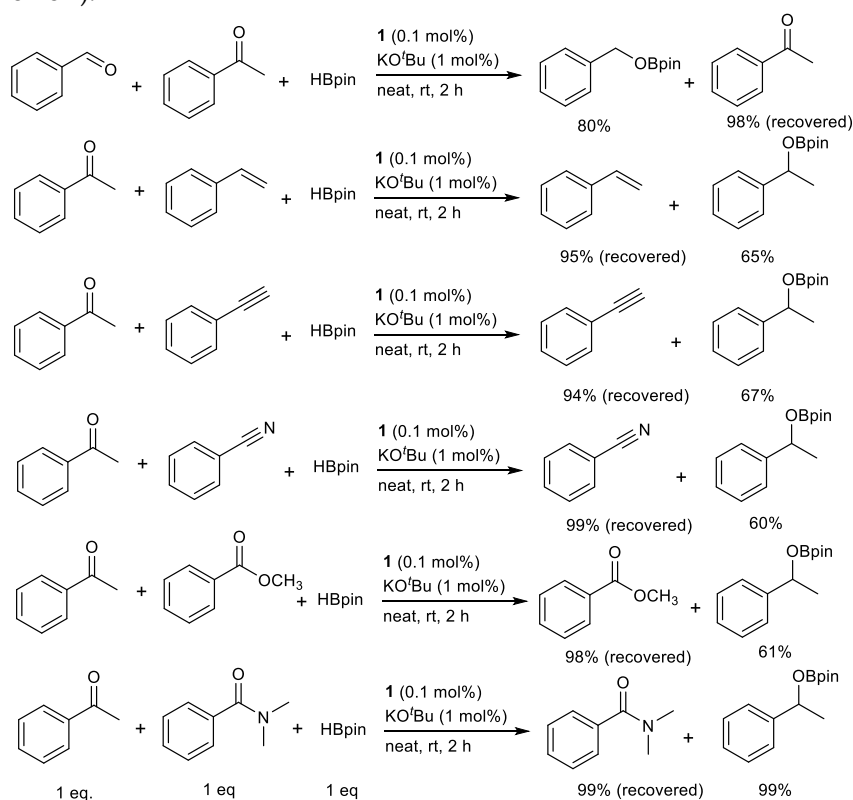
3.3. Chemoselectivity

Chemoselectivity is a critical issue when a catalyst is considered to be used in practical process. To establish the chemoselectivity of the present catalyst for ketone and other reducible chemicals, we conducted several additional experiments to evaluate the present catalyst. Thus, several parallel reactions were set up while using two mixed substrates under the standard catalytic conditions as shown in Scheme 2. First, equimolar acetophenone and benzaldehyde was used to react with 1 equiv. of HBpin in the presence of **1**/KO*t*Bu under neat conditions, and it was found that hydroboration selectively occurred on the aldehyde with 90% yield and the ketone was fully recovered. Likewise, competing experiments using equimolar acetophenone and other reducible chemicals such alkene, alkyne, nitrile, ester and amide were performed. The results reveal that in all cases the hydroboration was chemoselective for ketone over other functional groups. Interestingly, while the presence of other reducible substrates affected the reaction of ketone hydroboration with lower yields, the tertiary amide was found not to interrupt the reaction at all (Scheme 2).

Scheme 2. Chemoselective hydroboration between ketone and other reducible substrates. Conditions: acetophenone (1.0 mmol), reducible substrate (1.0 mmol), **1** (0.1 mol%), KO*t*Bu (1 mol%) and HBpin (1.0 mmol), neat, rt, 2 h.

4. Conclusions

In conclusion, we have synthesized and characterized a novel supramolecular framework (**1**) by the self-assembly of a pyridine-based hydrazide-hydrazone ligand (**L**) and Co(NCS)$_2$. X-ray structural analysis has determined the molecular structure to be a 3-D framework resulting from the hydrogen-bonding packing between 2-D sheets of the extended coordination between **L** and metal ions. The catalytic applications of the as-synthesized polymeric materials in combination with an activator for hydroboration (and hydrosilylation) reactions of ketones and aldehydes were explored. The results suggest that **1** can be employed for both hydroboration and hydrosilylation catalysis for ketones and aldehydes under mild conditions, albeit it is not a viable catalyst for alkene and alkyne hydrofunctionalization. Good chemoselectivity of this catalyst system was also observed

for aldehyde over ketone as well as ketone over other reducible groups such as alkene, alkyne, nitrile, ester and amide.

References

1. Gangu, K.K.; Maddila, S.; Mukkamala, S.B.; Jonnalagadda, S.B. A Review on Contemporary Metal-Organic Framework Materials. *Inorg. Chim. Acta* **2016**, *446*, 61-74.
2. Cai, G., Yan, P., Zhang, L., Zhou, H.C.; Jiang, H.L., Metal–organic framework-based hierarchically porous materials: Synthesis and applications. *Chem. Rev.*, **2021**, *121*, 12278-12326.
3. Chakraborty, G., Park, I.H., Medishetty, R.; Vittal, J.J., Two-dimensional metal-organic framework materials: synthesis, structures, properties and applications. *Chem. Rev.* **2021**, *121*, 3751-3891.
4. S. Kitagawa, K. Uemura. Dynamic porous properties of coordination polymers inspired by hydrogen bonds. *Chem. Soc. Rev.* **2005**, 34, 109-119.
5. MacDonald, J.C.; Dorrestein, P.C.; Pilley, M.M.; Foote, M.M.; Lundburg, J.L.; Henning, R.W.; Schultz, A.J.; Manson, J.L., Design of Layered Crystalline Materials Using Coordination Chemistry and Hydrogen Bonds. *J. Am. Chem. Soc.* **2000**, *122*, 11692-11702.
6. Cui, Y.; Ngo, H.L.; White, P.S.; Lin, W., Hierarchical Assembly of Homochiral Porous Solids Using Coordination and Hydrogen Bonds. *Inorg. Chem.* **2003**, *42*, 652-654.
7. Wu, X; Wang, J.; Huang, J.; Yang, S.; Robust, Stretchable, and Self-Healable Supramolecular Elastomers Synergistically Cross-Linked by Hydrogen Bonds and Coordination Bonds. *ACS appl. Mater. Interf.* **2019**, *11*, 7387-7396.
8. Kwon, H.; Lee, E. Coordination preference of hexa(2-pyridyl)benzene with copper(II) directed by hydrogen bonding. *CrystEngComm* **2018**, *20*, 5233-5240.
9. Chang, C.C.; Kinjo, R. Catalytic Hydroboration of Carbonyl Derivatives, Imines, and Carbon Dioxide. *ACS Catal.* **2015**, *5*, 3238-3259.
10. Cho, B.T., Recent development and improvement for boron hydride-based catalytic asymmetric reduction of unsymmetrical ketones. *Chem. Soc. Rev.* **2009**, *38*, 443–452.
11. Wang, W.; Lu, K.; Qin, Y.; Yao, W.; Yuan, D.; Pullarkat, S.A; Xu, L.; Ma, M, Grignard reagents-catalyzed hydroboration of aldehydes and ketones. *Tetrahedron*, **2020**, 76, 131145.
12. Tamang, S. R.; Findlater, M., Emergence and Applications of Base Metals (Fe, Co, and Ni) in Hydroboration and Hydrosilylation. *Molecules*, **2019**, *24*, 3194.
13. Wang, R.; Park, S., Recent Advances in Metal-Catalyzed Asymmetric Hydroboration of Ketones. *ChemCatChem*, **2021**, *13*, 1898-1919.
14. Shegavi, M.L.; Bose, S.K., Recent advances in the catalytic hydroboration of carbonyl compounds. *Catal. Sci. Tech.*, **2019**, *9*, 3307-3336.
15. Jakhar, V.K., Barman, M.K.; Nembenna, S., Aluminum monohydride catalyzed selective hydroboration of carbonyl compounds. *Organic letters*, **2016**, *18*, 4710-4713.
16. Oluyadi, A.A., Ma, S.; Muhoro, C.N., Titanocene(II)-Catalyzed Hydroboration of Carbonyl Compounds. *Organometallics*, **2013**, *32*, 70-78.
17. Baishya, A., Baruah, S.; Geetharani, K., Efficient hydroboration of carbonyls by an iron(II) amide catalyst. *Dalton Transactions*, **2018**, *47*, 9231-9236.
18. Khoo, S., Cao, J., Ng, F.; So, C.W., Synthesis of a Base-Stabilized Silicon(I)–Iron(II) Complex for Hydroboration of Carbonyl Compounds. *Inorg. chem.*, **2018**, *57*, 12452-12455.

19. Vijjamarri, S., O'Denius, T.M., Yao, B., Kubátová, A.; Du, G., Highly Selective Hydroboration of Carbonyls by a Manganese Catalyst: Insight into the Reaction Mechanism. *Organometalics*, **2020**, *39*, 3375-3383.

20. Li, M., Liu, X.; Cui, D., Catalytic hydroboration of carbonyl derivatives by using phosphinimino amide ligated magnesium complexes. *Dalton Trans.*, **2021**, *50*, 13037-13041.

21. Kim, J.H., Jaladi, A.K., Kim, H.T.; An, D.K., Lithium tert-Butoxide-catalyzed Hydroboration of Carbonyl Compounds. *Bull. Kor. Chem. Soc.*, **2019**, *40*, 971-975.

22. Zhang, G., Zeng, H., Wu, J., Yin, Z., Zheng, S. and Fettinger, J.C., Highly Selective Hydroboration of Alkenes, Ketones and Aldehydes Catalyzed by a Well-Defined Manganese Complex. *Angew. Chem. Int. Ed.* **2016**, *55*, 14369-14372.

23. G. Zhang, J. Wu, H. Zeng, M.C. Neary, M. Devany, S. Zheng, P.A. Dub. , Dearomatization and Functionalization of Terpyridine Ligands Leading to Unprecedented Zwitterionic Meisenheimer Aluminum Complexes and Their Use in Catalytic Hydroboration. *ACS Catal*. **2019**, *9*, 874-884.

24. G. Zhang, J. Wu, S. Zheng, M.C. Neary, J. Mao, M. Flores, R.J. Trovitch, P.A. Dub. Redox-Noninnocent Ligand-Supported Vanadium Catalysts for the Chemoselective Reduction of C＝X (X= O, N) Functionalities. *J. Am. Chem. Soc.* **2019**, *141*, 15230-15239.

25. Ma, D.H., Jaladi, A.K., Lee, J.H., Kim, T.S., Shin, W.K., Hwang, H.; An, D.K., Catalytic Hydroboration of Aldehydes, Ketones, and Alkenes Using Potassium Carbonate: A Small Key to Big Transformation. *ACS omega*, **2019**, *4*, 15893-15903.

26. Nowicki, M., Kuciński, K., Hreczycho, G. and Hoffmann, M., Catalytic and non-catalytic hydroboration of carbonyls: Quantum-chemical studies. *Org. Biomol. Chem.*, **2021**, *19*, 3004-3015.

27. Bage, A.D., Nicholson, K., Hunt, T.A., Langer, T.; Thomas, S.P., The Hidden Role of Boranes and Borohydrides in Hydroboration Catalysis. *ACS Catal.*, **2020**, *10*, 13479-13486.

28. J. Wu, H. S. Zeng, J. Cheng, S. P. Zheng, J. A. Golen, D. R. Manke, G. Zhang, Cobalt(II) coordination polymer as a precatalyst for selective hydroboration of aldehydes, ketones, and imines. *J. Org. Chem*. **2018**, *83*, 9442-9448.

29. G. Zhang, J. Wu, S. Li, S. Cass, S. Zheng, Markovnikov-Selective Hydroboration of Vinylarenes Catalyzed by a Cobalt (II) Coordination Polymer. *Org. Lett*. **2018**, *20*, 7893-7897.

30. G. Zhang, S. Li, J. Wu, H. Zeng, Z. Mo, K. Davis and S. Zheng, Highly efficient and selective hydroboration of terminal and internal alkynes catalysed by a cobalt(II) coordination polymer. *Org. Chem. Front*. **2019**, *6*, 3228-3233.

31. G. Zhang, J. Cheng, K. Davis, M.G. Bonifacio, C. Zajaczkowski, Practical and selective hydroboration of aldehydes and ketones in air catalysed by an iron(II) coordination polymer. *Green Chem*. **2019**, *21*, 1114-1121.

32. E. Liu, L. Li, J. Cheng, G.Zhang, Synthesis and structural characterization of dinuclear Zinc(II) and Europium(III) complexes based on a bis-hydrazone ligand. *J. Mol. Struct*. **2019**, *1188*, 1-6.

33. L. Li, Y.Z. Zhang, C. Yang, E. Liu, J.A. Golen, A.L. Rheingold, G. Zhang, Synthesis and structural characterization of zinc(II) and cobalt (II) complexes based on multidentate hydrazone ligands. *J. Mol. Struct*. **2016**, *1110*, 180-184.

34. B. Parmar, Y. Rachuri, K. K. Bisht, E. Suresh, Mixed-Ligand LMOF Fluorosensors for Detection of Cr(VI) Oxyanions and Fe^{3+}/Pd^{2+} Cations in Aqueous Media. *Inorg. Chem.* **2017**, 56, 10939-10949.

35. K. Roztocki, D. Jędrzejowski, M. Hodorowicz, I. Senkovska, S. Kaskel, D. Matoga, Effect of Linker Substituent on Layers Arrangement, Stability, and Sorption of Zn-Isophthalate/Acylhydrazone Frameworks. *Cryst. Growth Des.* **2018**, *18*, 488-497.

36. Sheldrick, G. M. SHELXTL, An Integrated System for Solving, Refining, and Displaying Crystal Structures from Diffraction Data; University of Göttingen, Göttingen, Federal Republic of Germany, 1981.

37. Sheldrick, G. M. Crystal Structure Refinement by SHELXL. *Acta Cryst*. **2015**, *A71*, 3-8.

38. Spek, A.L. 2005, PLATON, A Multipurpose Crystallographic Tool, Utrecht University, Utrecht, The Netherlands.

39. Spek, A.L. *J. Appl. Cryst*. **2003**, *36*, 7-13.

40. Liu, X.L., Fan, W.W., Lu, Z.X., Qin, Y., Yang, S.X., Li, Y., Liu, Y.X., Zheng, L.Y.; Cao, Q.E., Solvent-Driven Reversible Phase Transition of a Pillared Metal–Organic Framework. *Chem. Eur. J.*, **2019**, *25*, 5787-5792.

41. Krūkle-Bērziņa, K., Belyakov, S., Mishnev, A.; Shubin, K., Stability and Phase Transitions of Nontoxic γ-Cyclodextrin-K⁺ Metal-Organic Framework in Various Solvents. *Crystals*, **2020**, *10*, 37.

42. Kundu, T., Wahiduzzaman, M., Shah, B.B., Maurin, G.; Zhao, D., Solvent-induced control over breathing behavior in flexible metal–organic frameworks for natural-gas delivery. *Angew. Chem. Int. Ed.*, **2019**, *58*, 8073-8077.